Life-Cycle of Structures and Infrastructure Systems – Biondini & Frangopol (Eds)

Optimal strengthening of masonry arch bridges with externally bonded reinforcing layers

M. Bruggi & A. Taliercio
Department of Civil and Environmental Engineering, Politecnico di Milano, Milan, Italy

ABSTRACT: Strengthening is a natural step following a failed bridge assessment. Referring to masonry bridges, a numerical tool is presented to find the optimal distribution of reinforcement to be externally bonded to two-dimensional elastic no-tension structural elements, with the aim of maximizing their overall stiffness. Notwithstanding the non-linearity of the adopted material model, no incremental procedure is needed to prescribe equilibrium of the strengthened element. Indeed, the same minimization procedure handles both the energy-based solution of the no-tension elastic body and the topology optimization problem that distributes the optimal reinforcement. A few numerical simulations are presented to assess the capabilities of the proposed procedure in defining the optimal reinforcement layouts for masonry arches and arch bridges, subjected to gravity loads and resting on fixed or elastic foundations. Designers can exploit the tool to sketch a preliminary layout of the FRP strengthening, which should be subsequently detailed according to technical codes.

1 INTRODUCTION

Externally bonded Fiber Reinforced Polymers (FRPs) are nowadays widely used to strengthen, upgrade, or retrofit deteriorated masonry structural elements (Foraboschi 2001, Grande et al. 2008). FRPs have several positive properties, including resistance to wear and corrosion, flexibility, high strength-to-weight ratio, etc. Unlike other materials (e.g., reinforced concrete and steel) that were widely used in the past to strengthen existing buildings, FRPs do not significantly increase the weight of the of the building and, as such, are extremely appropriate in seismic regions (Shrive 2006). FRPs compensate the limited tensile strength of masonry, and increase the load-carrying capacity and ductility of the repaired structural element, as experimentally and numerically shown by several authors (see e.g. Caporale & Luciano 2012).

Drawbacks related to the use of FRPs as retrofitting materials for masonry structures are the possibility of debonding, which can nullify the effectiveness of the reinforcement (see e.g. Capozucca 2010, 2011), or worsening in crack diffusion in the unreinforced regions (Angelillo et al. 2014). Debonding can be avoided by appropriate surface treatments, using fasteners, or applying carbon FRP plates at the intrados of masonry arches, rather than strips or sheets, as suggested by Borri et al. (2011).

According to these remarks, the interest in obtaining methodologies suitable to identify effective reinforcing layouts for masonry constructions under given load conditions is apparent. Some authors basically propose to arrange the reinforcement according to a strut-and-tie scheme, either in such a way as to heal the cracks formed in the unreinforced element (Li et al. 2013), or using optimization procedures (Krevaikas & Triantafillou 2005). A simple strut-and-tie scheme, however, might not be the most appropriate one to retrofit elements of complex geometry, or subjected to nontrivial load conditions. Accordingly, Bruggi & Taliercio (2013) and Bruggi et al. (2013) proposed a general approach based on Topology Optimization (TO - see e.g. Bendsøe & Kikuchi 1988) for 2D, in-plane loaded structural elements, to obtain reinforcing layouts that

DOI: 10.1201/9781003323020-161

minimize a suitable maximum equivalent stress for a prescribed amount of reinforcement. A similar approach was later proposed by Cunha & Chaves (2014) and Bruggi & Taliercio (2015a) for transversely loaded 2D structural elements. In these papers, the optimal reinforcing layout maximizes the elastic stiffness of the reinforced element for a given amount of fiber reinforcement; in the latter paper, the anisotropic and unsymmetric behavior in tension and compression of the reinforcing layers is also taken into account.

Recently, Bruggi & Taliercio (2017) proposed an approach to define the optimal fiber-reinforcement of 2D structural elements made of no–tension materials (e.g. plain concrete or masonry). Here, this approach is specialized to masonry arches and arch bridges that have to be retrofitted by externally bonded FRP strips. The reinforcement is supposed to be unable to carry compressive stresses. A TO formulation is presented to distribute a prescribed amount of fiber-reinforcement at either the intrados or the extrados of the arch, or at both sides, to maximize the overall elastic stiffness of the strengthened element. Unlike the papers quoted above, where the structural elements to be reinforced are linearly elastic, a no-tension model is used to account for the negligible tensile strength of the material. The stress analysis of the no-tension element is itself reduced to a TO problem, according to the approach recently proposed by Bruggi (2014). Indeed, following Del Piero (1989), masonry is supposed to be a hyperelastic, no-tension material. The possible anisotropy associated with the brickwork bond is neglected, and masonry behaves isotropically if all the principal stresses are strictly negative (compressive). The occurrence of positive (tensile) principal stresses is prevented by replacing the isotropic material by an equivalent, orthotropic material whose elastic constants depend on the principal stresses and on the orientation of the principal stress directions. Hyperelasticity allows the equilibrium of the body to be enforced by solving a topology optimization problem, i.e. finding the distribution of the equivalent orthotropic material that minimizes the overall strain energy of the no–tension body.

The main advantage of the approach proposed here is that both the analysis of the no–tension solid and the definition of the layout of the optimal no-compression reinforcement are embedded within the same minimization procedure.

Following Amir & Sigmund (2013) and Gaynor et al. (2013), a combined truss–continuum approach is adopted to model the strengthened element.

2 EQUILIBRIUM OF NO-TENSION BODIES AS A TOPOLOGY OPTIMIZATION PROBLEM

Consider a 2D no-tension isotropic solid, occupying a volume Ω. Typically, the solid can be made of plain concrete or masonry: in the latter case, the macroscopic anisotropy of the material is neglected, as the tensile strength of masonry is actually negligible only perpendicularly to the joints. Mathematical formulations aimed at analyzing no-tension materials were proposed by several authors since the '80s of last century (see e.g. Giaquinta & Giusti 1985, Del Piero 1989, Cuomo & Ventura 2000). More recently, Angelillo et al. (2010) proposed to analyze no-tension solids by replacing the real material by an 'equivalent' orthotropic material that exhibits negligible stiffness in any direction along which the principal stresses in the real medium are non-negative. This idea was later exploited by Bruggi (2014) to re-formulate the analysis of 2D no-tension solids as a TO problem: the distribution of the equivalent material is obtained by minimizing the strain energy of the solid. This non-incremental approach provides the solution under given loads through a one-shot energy-based optimization procedure, provided that the applied loads are compatible with the no-tension constraint. The collapse load of no-tension 2D solids can also be determined by an algorithm based on the approach outlined above (Bruggi & Taliercio 2015b).

The problem formulation is only briefly recalled hereafter; further details can be found in the papers referred above. Let $\mathbf{t}_0$ denote tractions prescribed over the free boundary of the solid, Γ_t, whereas $\mathbf{u}_0$ denote displacements prescribed over the constrained boundary, Γ_u. Also, let (z_1, z_2) be the symmetry axes of the equivalent orthotropic material. These axes are assumed to be locally aligned with the directions (z_I, z_{II}) of the principal stresses (σ_I, σ_{II}) at any point of the real

solid, to maximize the material stiffness (Pedersen 1989). Let θ denote the angle between (z_I, z_{II}) and the axes of a given Cartesian reference system. In weak form, the problem solution can be sought as follows:

$$\begin{cases} \min\limits_{\rho_1,\rho_2} & \frac{1}{2}\int_\Omega \mathbf{D}(\rho_1,\rho_2,\theta) : \varepsilon(\mathbf{u}) : \varepsilon(\mathbf{u}) d\Omega \\ \text{s.t.} & \int_\Omega \mathbf{D}(\rho_1,\rho_2,\theta) : \varepsilon(\mathbf{u}) : \varepsilon(\mathbf{v}) d\Omega = \int_{\Gamma_t} \mathbf{t}_0 \cdot \mathbf{v} d\Gamma \ \forall \mathbf{v}, \\ & \mathbf{u}|_{\Gamma_u} = \mathbf{u}_0, \\ & \theta \text{ s.t. } z_1 = z_I \text{ and } z_2 = z_{II}, \\ & \rho_1,\rho_2 \text{ such that } \sigma_I \le 0 \text{ and } \sigma_{II} \le 0, \\ & 0 < \rho_{min} \le \rho_1,\rho_2 \le 1, \end{cases} \tag{1}$$

where $\mathbf{u}$ denotes the (infinitesimal) displacement field, $\varepsilon(\mathbf{u})$ is the (infinitesimal) strain tensor, $\mathbf{D}$ is the fourth-order elasticity tensor of the equivalent orthotropic material, and ρ_1, ρ_2 are nondimensional parameters defined hereafter. In plane stress conditions, and using Voigt's notation, the matrix of the elastic stiffness constants in the material reference frame (z_1,z_2) can be expressed as

$$[D] = \frac{1}{1-\nu_m^2}\begin{bmatrix} \widetilde{E}_1 & \widetilde{\nu}_{12}\widetilde{E}_2 & 0 \\ \widetilde{\nu}_{21}\widetilde{E}_1 & \widetilde{E}_2 & 0 \\ 0 & 0 & \widetilde{G}_{12}(1-\nu_m^2) \end{bmatrix}, \tag{2}$$

where $\widetilde{E}_i$ (i = 1, 2) are the Young's moduli of the orthotropic equivalent material, $\widetilde{G}_{12}$ its shear modulus, $\widetilde{\nu}_{12}, \widetilde{\nu}_{21}$ its Poisson's ratios (with $\widetilde{\nu}_{12}/\widetilde{E}_1 = \widetilde{\nu}_{21}/\widetilde{E}_2$). To prevent the principal stresses from being positive in the equivalent solid, the stiffness of the orthotropic material is prescribed to vanish along the direction(s) of the tensile principal stress(es) in the real solid. To avoid numerical instabilities, the elastic constants of the equivalent material are related to those (E_m, v_m) of the real isotropic material according to a generalization of the so-called SIMP model (Bendsøe & Sigmund, 1999), which reads

$$\widetilde{E}_i = \rho_i^p E_m, \quad \widetilde{\nu}_{ij} = \sqrt{\frac{\rho_i^p}{\rho_j^p}}\nu_m, \quad \widetilde{G}_{12} = \sqrt{\rho_1^p \rho_2^p}\frac{E_m}{2(1+\nu_m)} \tag{3}$$

for i, j = 1, 2. The parameters ρ_i (i = 1, 2) range from a strictly positive value ρ_{min} to 1 (see Eq. (1)), the extreme values corresponding to a negligible stiffness or a non-penalized stiffness along z_i, respectively, depending on the sign of the relevant principal stress; these parameters can be interpreted as 'nondimensional material densities' along the symmetry axes of the orthotropic solid. A strictly positive lower bound is prescribed, to avoid singularity of the stiffness matrix in a finite-element formulation. p is a penalization parameter, usually taken equal to 3 (Bendsøe & Sigmund, 1999).

The expressions of the equivalent constants in Eq. (3) are similar to those proposed by Cordebois & Sidoroff (1982) for anisotropic damaged materials, thus considering the penalization of the elastic constants as a form of tensile damage.

3 OPTIMAL FIBER-REINFORCEMENT OF 2D NO-TENSION BODIES

Assume now that the no-tension solid has to be retrofitted by unidirectional FRP layers. These layers are assumed to withstand only tensile stresses along the fibers. A given amount of reinforcement, V_f, normalized to the maximum amount that can be bonded over the entire free boundary of the body, is prescribed. A minimization problem is formulated to find the optimal distribution of reinforcement that maximizes the stiffness of the strengthened body. The no-compression constraint is enforced using a SIMP-type approach similarly to Eq. (3).

The solution of the nonlinear equilibrium problem for the reinforced body is sought by embedding the minimization procedure within the energy-based approach presented in the previous Section: the discretized FE form of the procedure is presented hereafter. A mesh made of N truss elements for the reinforcement layers, and M four-node plane elements for the underlying no-tension solid, is used. The non-dimensional densities used to enforce the no-tension constraint in the original solid and the no-compression constraint in the reinforcement are assumed to be element-wise constant. In the j-th truss-like element the density of the reinforcement is denoted by x_j, whereas in the i-th plane element the densities that govern the stiffness of the 'equivalent material' along its symmetry axes are denoted by x_{1i}, x_{2i}. The orientation of the material symmetry axes of the i–th FE with respect to the global Cartesian reference frame is denoted by θ_i.

The stiffness matrix of the j-th truss element can be expressed as $x_j^p \mathbf{K}_{0j}$, where $\mathbf{K}_{0j}$ is the stiffness matrix if the element undergoes tensile stresses (so that $x_j = 1$). The stiffness matrix of the i-th plane element will be denoted by $\mathbf{K}_i(x_{1i}, x_{2i}, \theta_i)$. The implemented discrete form of the problem formulated above reads:

$$
\begin{cases}
\min\limits_{x_j, x_{1i}, x_{2i}} & \mathcal{C} = \\
\text{s.t.} & \sum\limits_{i=1}^{M} \mathbf{U}_i^T \mathbf{K}_i(x_{1i}, x_{2i}, \theta_i)\mathbf{U}_i + \sum\limits_{j=1}^{N} \mathbf{U}_j^T x_j^p \mathbf{K}_{0j}\mathbf{U}_j \\
& \sum_{i=1}^{M} \mathbf{K}_i(x_{1i}, x_{2i}, \theta_i)\mathbf{U}_i + \sum_{j=1}^{N} x_j^p \mathbf{K}_{0j}\mathbf{U}_j = \mathbf{F}, \\
& \theta_i \text{ such that } z_1 = z_I \text{ and } z_2 = z_{II}, \\
& x_{1i}, x_{2i} \text{ such that } \sigma_{i,I} \leq 0 \text{ and } \sigma_{i,II} \leq 0, \\
& 0 < \rho_{min} \leq x_{1i},\ x_{2i} \leq 1,\ i = 1 \ldots M \\
& x_j \text{ such that } \sigma_j \geq 0, \\
& 0 \leq x_j \leq 1,\ j = 1 \ldots N \\
& \dfrac{\sum_{j=1}^{N} x_j A_j}{\sum_{j=1}^{N} A_j} \leq V_f,
\end{cases}
\tag{4}
$$

where $\mathbf{U}_i$, $\mathbf{U}_j$ are the arrays of the d.o.f.s of the 2D and the truss-like finite elements, respectively; $\mathbf{F}$ is the array of the equivalent nodal loads.

In Eq. (4), the objective function is the structural compliance C, i.e. the work of the external loads at equilibrium. The overall strain energy (half of the structural compliance C) is the sum of that stored in the underlying no–tension material and in the fiber–reinforcement to be optimized. Note that the adopted objective function is the same suggested by building codes (EN 1992-1-1, 2004) to derive optimal reinforcement layouts for r.c. members.

In Eq. (4), the constraints in Eq. (1) are reported in discretized form. Additionally, the third last constraint avoids the presence of any strengthening material carrying compressive stresses. The second-last constraint concerns the reinforcement density in any truss element, which is allowed to vanish if the element undergoes compressive stresses. Finally, the last constraint enforces an upper bound on the volume of reinforcement, depending on the area of each truss element, A_j, and the relevant density.

The constrained minimum compliance problem stated in Eq. (4) can be numerically solved by the so–called Method of Moving Asymptotes (MMA – see e.g. Svanberg, 1987). This gradient-based method uses sequential convex programming and the analytical computation of the sensitivities of the objective function. At each iteration, the MMA solves a sequence of simpler approximate sub-problems, which are separable, convex and constructed according to the sensitivity information at the current step, as well as to the iteration history. This approach has been found to be effective in solving large-scale TO problems, giving results in agreement with those achieved through optimality criteria, see e.g. Bendsøe & Sigmund (2003).

The stress constraints in Eq. (4) are enforced by implementing the penalization approach proposed by Ananiev (2005), with the main aim of reducing the computational effort related to the implementation of clusters of local stress constraints. Whenever a principal stress is found to be positive in any element i of the no-tension material, or the stress is found to be

negative in any element j of the reinforcing layer, the corresponding design variables are penalized, and a modified compliance $\widehat{\mathcal{C}}$ is computed. The penalized densities are defined as

$$\begin{aligned} &\widehat{x}_{1i} = kx_{1i},\ \widehat{x}_{2i} = kx_{2i},\ i = 1 \ldots M, \\ &\widehat{x}_j = kx_j,\ j = 1 \ldots N, \end{aligned} \tag{5}$$

where k < 1 is a penalization factor (herein k = 0.5). This heuristic approach was shown to be effective in the treatment of stress constraints (Ananiev, 2005).

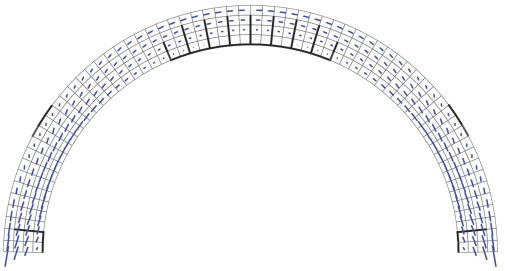

Figure 1. Optimal fiber-reinforcement of a single arch made of linear elastic NT material: the principal compressive stresses in the strengthened element are also shown.

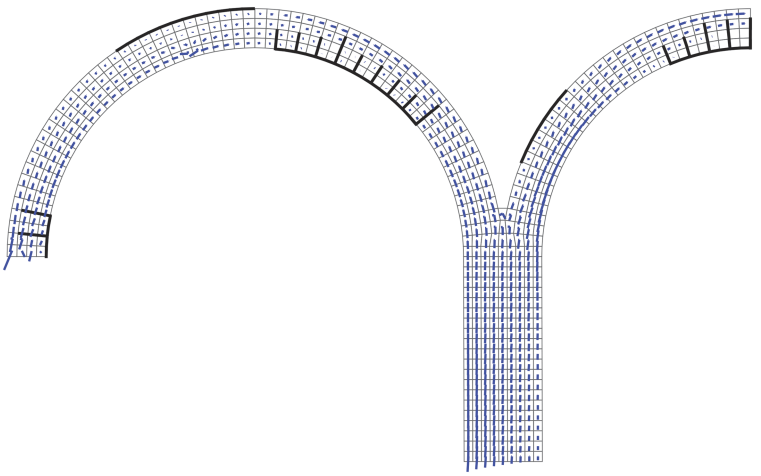

Figure 2. Optimal fiber-reinforcement of a three-span arch bridge made of linear elastic NT material resting on rigid supports: the principal compressive stresses in the strengthened element are also shown.

Providing the MMA with the reduced objective function $\widehat{\mathcal{C}}$ and the relevant sensitivities, the gradient–based minimizer updates the design variables $x_{1i,}\ x_{2i}$ ($i = 1 \ldots M$) and x_j ($j = 1 \ldots N$), and prevents any stiff material to exist along the weak direction(s) of the no-tension body, as well as any compressed reinforcement element. Computing the sensitivities of the reduced objective function $\widehat{\mathcal{C}}$ with respect to the minimization unknowns is straightforward (see Bruggi & Taliercio, 2017).

4 NUMERICAL APPLICATIONS

In the numerical applications shown hereafter, attention is focused on the reinforcement of arch-like structural elements. The elastic properties of the no-tension isotropic material are E_m = 4,500 MPa

and v_m = 0.2. The thickness of the FRP layer is th_r = 1.40 mm, whereas the elastic modulus of the reinforcement is E_r = 205,000 MPa.

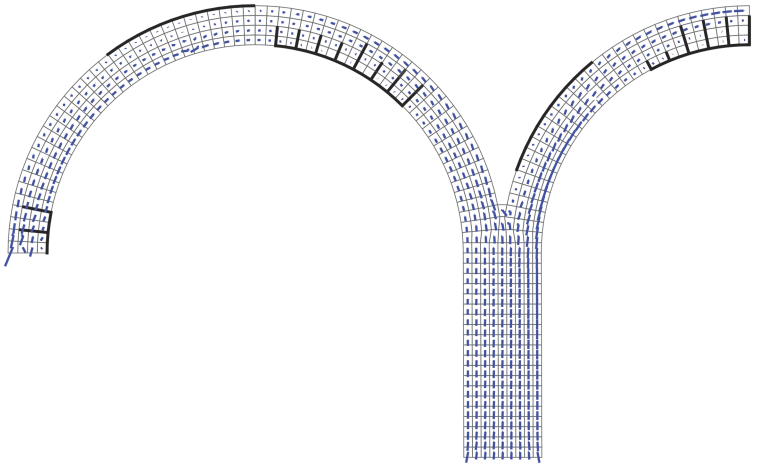

Figure 3. Optimal fiber-reinforcement of a three-span arch bridge made of linear elastic NT material assuming the pier to rest on an elastic support: the principal compressive stresses in the strengthened element are also shown.

First of all, a single semi-circular arch, with an external radius of R_{em} = 4.75 m, an internal radius of R_{em} = 4.00 m, and an out–of–plane thickness of t_{hm} = 1 m, is considered. The arch undergoes its self-weight, being $\gamma_m = 18\ kN/m^3$ the unit weight, and the weight of an infill up to the top of the extrados of the arch, being $\gamma_i = \gamma_m$ the unit weight of the added material.

The optimal layout of two tension-only reinforcing layers, which can be located along the intrados and/or the extrados of the arch, is sought. To make the fiber-reinforcement at the intrados effective, tension-resistant fasteners must be provided to connect the reinforcement to the inner (compressed) part of the body. Otherwise, radial tensile stresses would occur and nullify adhesion. A maximum volume fraction of reinforcement V_f = 0.5 is prescribed.

Figure 1 shows the optimal reinforcement, along with the principal compressive stresses in the strengthened specimen. The FRP layers are located at the crown, where a cracked area is found, at the intrados of the abutments, and at the extrados of the haunches. Note the presence of fasteners around the crown, to fulfil equilibrium of the reinforcing curved layer. Fasteners also help the flow of the compressive stresses deviate towards the bulk of the no-tension body, as shown by the orientation of the principal stesses at the abutments. It must be noticed that the overall amount of distributed reinforcement is less than V_f. The need to consider a volume fraction stems from the use of a topology optimization formulation, having the aim of limiting the amount of reinforcement to be used. In this example and those that follow, the no-compression requirement for the FRP layers prevents the optimizer from exploiting any compressive reinforcement to improve the overall stiffness. Hence, the upper bound becomes active depending on the values of V_f.

Then, a three-span arch bridge is considered, assuming that each span has the same geometry as the arch investigated above and that the same loads (gravity and fill) are applied. Symmetry is exploited, and only the left part of the bridge (including an arch, half of the central span, and the supporting pier) is analyzed. The rectangular pier has a base 1.50 m wide and is 4.00 m high. In Figure 2 the layout of the optimal fiber-reinforcement and the principal compressive stresses in the strengthened element are shown, assuming the supports to be fixed. The optimal reinforcement of the central arch is quite similar to that of the single arch, see Figure 1. However, both the location and the extension of the reinforcing layers of the outer arch are remarkably different. Thus, modeling the entire bridge is an essential task to achieve an effective strengthening.

As a peculiar feature of the adopted linear elastic no-tension model, elastic supports may be straightforwardly introduced in the numerical simulations. In Figure 3, the optimal layout of the fiber-reinforcement in the same three-span arch is presented, along with the principal compressive stresses in the strengthened element, assuming now the base of the pier to rest on an elastic foundation, with a modulus of subgrade reaction $k_P = 0.1\ N/mm^3$. This accounts for the deformability of the supporting foundation and the underlying soil. Compared to the case of fixed support shown in Figure 2, a more homogeneous stress distribution is found at the base of the pier. Concerning the optimal layout of the reinforcing layers, minor modifications are found in the outer arch, whereas a larger amount of reinforcement is used in the central one.

5 CONCLUSIONS

A theoretical formulation based on Topology Optimization has been proposed to define the optimal layout of a given amount of reinforcement to be applied on 2D masonry arch-like structural elements to maximize their stiffness. Assuming masonry to be an elastic, isotropic, no–tension material and FRPs to resist only tensile stresses, the formulation simultaneously avoids principal tensile stresses in the arch and compressive stresses in the reinforcement.

The main advantage of the proposed approach is that no incremental procedure is needed to compute the objective function, notwithstanding the inherent non–linearity of the adopted material model. The same minimization procedure deals with both the energy–based analysis of the no–tension elastic body, and the topology optimization problem that distributes the optimal reinforcement.

The examples presented in Section 4 show that when FRP strips are used to retrofit no-tension arches, fasteners are required at the intrados: otherwise, any reinforcement would be simply blown out, owing to the inability of the material to withstand radial tensile stresses. In all the applications, smooth convergence of the objective function was found in a reasonable number of iterations. Also, soil deformability was found to affect the optimal reinforcing layout (compare Figures 2 and 3).

The implementation described in this contribution considers a single load case, meaning that it is directly applicable to long span masonry arch bridges, where live loads are small in comparison to dead loads. When small and medium-span bridges are addressed, multiple load cases must be considered. This may be done by optimizing separately for each one of the relevant load cases and, then, looking at the envelope of the achieved solutions as the effective reinforcement to be used. However, this procedure does not guarantee that the amount of reinforcement is less than the prescribed volume fraction. To overcome this issue, a single optimization procedure may be implemented adopting as objective function a weighted sum of the strain energy for each one of the load cases, while taking into full account the volume constraint.

In the continuation of the research, an extension of the formulation to 3D no-tension solids is planned. The aim is to propose optimal reinforcing layouts for masonry vaults of any geometry, typically groin, rib, and domical vaults, possibly including lunettes. Refined finite element meshes, or higher-order finite elements, are expected to be required to obtain meaningful solutions, with a dramatic increase in computational cost compared to 2D problems. On the other hand, the possibility of avoiding incremental solutions is expected to make the proposed numerical approach more robust and less expensive than 'classical' optimization procedures for nonlinear bodies.

REFERENCES

Amir, O. & Sigmund, O. 2013. Reinforcement layout design for concrete structures based on continuum damage and truss topology optimization. *Struct. Multidisc. Optim.* 47(2): 157–174.

Ananiev, S. 2005. On equivalence between optimality criteria and projected gradient methods with application to topology optimization problem. *Multibody System Dynamics* 13(1):25–38.

Angelillo, M., Cardamone, L. & Fortunato, A. 2010. A numerical model for masonry-like structures. *J. Mech. Mater. Struct.* 5(4):583–615.

Angelillo, M., Babilio, E., Cardamone, L., Fortunato, A. & Lippiello, M. 2014. Some remarks on the retrofitting of masonry structures with composite materials. *Compos. Part B: Eng*. 61:11–16.
Bendsøe, M.P. & Kikuchi, N. 1988. Generating optimal topologies in structural design using a homogeneization method. *Comp. Meth. Appl. Mech. Eng*. 71:197–224.
Bendsøe, M.P. & Sigmund, O. 1999. Material interpolation schemes in topology optimization. *Arch. Appl. Mech*. 69(9-10):635–654.
Bendsøe, M.P. & Sigmund, O. 2003. *Topology Optimization - Theory, Methods and Applications*. Springer, Berlin.
Borri, A., Castori, G. & Corradi M. 2011. Intrados strengthening of brick masonry arches with composite materials. *Compos. Part B: Eng*. 42(5):1164–1172.
Bruggi, M. 2014. Finite element analysis of no-tension structures as a topology optimization problem. *Struct. Multidisc. Optim*. 50(6):957–973.
Bruggi. M., Milani, G. & Taliercio, A. 2013. Design of the optimal fiber-reinforcement for masonry structures via topology optimization. *Int. J. Solids Struct*. 50(13):2087–2106.
Bruggi, M. & Taliercio, A. 2013. Topology optimization of the fiber-reinforcement retrofitting existing structures. *Int. J. Solids Struct*. 50(1):121–136.
Bruggi, M. & Taliercio, A. 2015a. Optimal strengthening of concrete plates with unidirectional fiber-reinforcing layers. *Int. J. Solids Struct*. 67-68:311–325.
Bruggi, M. & Taliercio, A. 2015b. Analysis of no-tension structures under monotonic loading through an energy-based method. *Comput. Struct*. 159:14–25.
Bruggi, M. & Taliercio, A. 2017. Optimal strengthening of no-tension structures with externally bonded reinforcing layers or ties. *Struct. Multidisc. Optim*. 55(5):1831–1846.
Caporale, A. & Luciano, R. 2012. Limit analysis of masonry arches with finite compressive strength and externally bonded reinforcement. *Compos. Part B: Eng*. 43(8):3131–3145.
Capozucca, R. 2010. Experimental FRP/SRP-historic masonry delamination. *Compos. Struct*. 92(4):891–903.
Capozucca, R. 2011. Experimental analysis of historic masonry walls reinforced by CFRP under in-plane cyclic loading. *Compos. Struct*. 94(1):277–289.
Cordebois, J.P. & Sidoroff, F. 1982. Anisotropic damage in elasticity and plasticity (in French). *J. Méc. Th. Appl*. special issue:45-60.
Cunha, J. & Chaves, L.P. 2014. The use of topology optimization in disposing carbon fiber reinforcement for concrete structures. *Struct. Multidisc. Optim*. 49(6):1009–1023
Cuomo, M. & Ventura, G. 2000. Complementary energy formulation of no tension masonry-like solids. *Comput. Methods Appl. Mech. Eng*. 189(1):313–339.
Del Piero, G. 1989. Constitutive equation and compatibility of the external loads for linear elastic masonry-like materials. *Meccanica* 24(3):150–162.
EN 1992- 1-1 2004. *Eurocode 2: Design of concrete structures - Part 1-1: General rules and rules for buildings*.
Foraboschi, P. 2001. Strength assessment of masonry arch retrofitted using composite reinforcements. *Masonry Int*. 15(1):17–25.
Gaynor, A.L., Guest, J.K. & Moen, C.D. 2013. Reinforced concrete force visualization and design using bilinear truss-continuum topology optimization. *J. Struct. Eng*. 139(4):607–618.
Giaquinta. M. & Giusti, E. 1985. Researches on the equilibrium of masonry structures. *Arch. Rat. Mech. An*. 88:359–392.
Grande, E., Milani, G. & Sacco, E. 2008. Modelling and analysis of FRP-strengthened masonry panels. *Eng. Struct*. 30(7):1842–1860.
Krevaikas, T.D. & Triantafillou, T.C. 2005. Computer-aided strengthening of masonry walls using fibre-reinforced polymer strips. *Mater. Struct*. 38(275):93–98.
Li, B., Qian, K. & Tran, C.T.N. 2013. Retrofitting earthquake-damaged RC structural walls with openings by externally bonded FRP strips and sheets. *J. Compos. Constr*. 17(2):259–270.
Pedersen, P. 1989. On optimal orientation of orthotropic materials. *Struct. Optim*. 1:101–106.
Shrive, N.G. 2006. The use of fibre reinforced polymers to improve seismic resistance of masonry. *Constr. Build. Mater*. 20(4):269–277.
Svanberg, K. 1987. Method of moving asymptotes - A new method for structural optimization. *Int. J. Numer. Methods Eng*. 24:359–373.